

1 **This preprint has not undergone peer review (when applicable) or any**
2 **post-submission improvements or corrections. The Version of Record of**
3 **this article is published in CELLULOSE, and is available online at**
4 **<https://doi.org/10.1007/s10570-021-04206-w>**

5 6 **Synergetic effect of cationic starch (ether/ester) and** 7 **Pluronic for improving inkjet printing quality of office** 8 **papers**

9
10 Mohit Sharma ^a, Roberto Aguado ^{b,*}, Dina Murtinho ^b, Artur J. M. Valente ^b, Paulo J. T. Ferreira ^a

11
12 ^a *University of Coimbra, CIEPQPF, Department of Chemical Engineering, Rua Sílvio Lima, Pólo II*
13 *– Pinhal de Marrocos, 3030-790 Coimbra, Portugal*

14 ^b *University of Coimbra, CQC, Department of Chemistry, Rua Larga, PT - 3004-535 Coimbra,*
15 *Portugal*

16
17 *rag@uc.pt (Roberto Aguado)

18 19 **Abstract**

20 Improving the printability of paper is still a relevant challenge, despite the fast development of digital communications.
21 While it is well-known that cationic starches enhance ink density, their commercial paper-grade forms are limited to
22 ethers with low degree of substitution. This work addresses the underexplored potential of highly substituted cationic
23 starch for paper coating and its combination with tri-block polymers, namely Pluronic (P123 and F127), taking
24 advantage of their supramolecular interactions with amylose chains. For that purpose, cationic starch ether and ester
25 (starch betainate), both with a degree of substitution of 0.3, were synthesized by alkaline etherification and by
26 transesterification, respectively. Paper without any surface treatment was subjected to one-side bar coating with
27 suspensions encompassing those products and Pluronic, besides other common components. Black, cyan, yellow and
28 magenta inks were printed on all coated papers through an inkjet printer. Key properties of printing quality such as the
29 gamut area, gamut volume, optical density, print-through, inter-color bleed and circularity were measured in a controlled
30 temperature-humidity environment. For instance, a formulation with cationic starch (ether/ester) and P123 improved the
31 gamut area by 16–18% in comparison to native starch-coated paper sheets. Interestingly, the individual assessment of

32 each component showed that cationic starch ether, starch betainate and P123 only improved the gamut area by 5.6%,
33 8.9% and 6.8%, respectively. Finally, but not less importantly, starch betainate was found to quench optical brightening
34 agents to a lesser extent than cationic starch ethers.

35

36 **Keywords**

37 *Cationic starch, Paper coating, Pluronics, Printing quality, Starch betainate, Whiteness*

38 **Introduction**

39 Paper coating formulations of printing and writing papers (P&W) often comprise a number of different components such
40 as pigments, surfactants, binders, thickeners, dispersants, crosslinkers, optical brightening agents (OBA), and/or
41 lubricants. In each case, the composition depends on which objectives papermakers set for the end product. A careful
42 selection of coating components can therefore be used to develop a paper surface with outstanding smoothness,
43 enhanced barrier properties and, receiving less attention in the literature, improved printing properties (Sharma et al.,
44 2020). Adsorption onto cellulosic fibers occurs when the paper surface is exposed to the coating suspension, but
45 manufacturers cannot neglect the interactions between the components of such suspension, which take place beforehand,
46 from the very moment they are mixed in an aqueous media. These interactions may include competitive adsorption,
47 inclusion complex formation, and stabilization/destabilization (Sousa, De Sousa, Reis, & Ramos, 2014).

48 The inkjet printing properties of fine papers are majorly influenced by the surface properties thereof, such as charge,
49 surface energy, roughness, permeability and surface strength (Bollström et al., 2013). A slight charge on the paper
50 surface may lead to the effective immobilization of the ink pigments onto the coated paper surface, whereas a certain
51 surface energy balance can favor a higher print density (Lundberg, Örtengren, Norberg, & Wågberg, 2010; Stankovská,
52 Gigac, Letko, & Opálená, 2014). Based on that, it has been shown that highly substituted cationic starch (HCS) has a
53 significant positive effect on the ink holdout (Lee et al., 2002), optical density, whiteness, water fastness and ink
54 fathening properties (Gigac, Stankovská, Opálená, & Pažitný, 2016; Lamminmäki, Kettle, & Gane, 2011). These
55 properties, along with the gamut area (GA), further increase in combination with amphiphilic polymers such as
56 poly(vinyl alcohol) (Baptista et al., 2016), most probably due to ease of interpolymer diffusion of ink carriers during
57 printing (Lamminmäki et al., 2011; Sousa et al., 2014).

58 While the biodegradability of native starch is obviously not under question, the biodegradability of its derivatives is too
59 often taken for granted. It has been shown that HCS ethers lose biodegradability with increasing degree of substitution
60 (DS), becoming non-biodegradable at $DS \geq 0.54$ (Bendoraitiene, Lekniute-Kyzike, & Rutkaite, 2018). In this context,
61 starch betainate (SB) rises as a convincing alternative, not only because betaine is naturally found, unlike conventional
62 cationizing reagents, but also because the ester bonds of SB are clearly more labile than ether bonds (Auzély-Velty &
63 Rinaudo, 2003). Likewise, starch betainate (SB), a cationic starch ester, was suggested for the improvement of paper
64 strength since the first work reporting its synthesis (Granö, Yli-Kauhaluoma, Suortti, Käki, & Nurmi, 2000). However,
65 as far as we know, no study has addressed the influence of SB on the printing properties of fine papers. This issue is
66 addressed in the present work, evaluating coating formulations comprising SB and other interesting amphiphilic
67 polymers, namely Pluronics.

68 Pluronics® is BASF's trade name for the less commonly called poloxamers. This trade name comprises non-ionic,
69 water-soluble, triblock copolymers of polyethylene oxide (PEO) and polypropylene oxide (PPO) units. Interestingly
70 enough, they generally form inclusion complexes with starch in aqueous solution. This kind of binding has a significant
71 effect on the dispersion performance and can be explained by hydrophobic interactions between hydrophobic parts of
72 Pluronics macromolecules and the cavities of the amylose helix (Petkova-Olsson, Altun, Ullsten, & Järnström, 2017).
73 Additionally, the micellar structure of these non-ionic surfactants also influences the adsorption onto the surface of
74 cellulosic materials, which is enhanced in the presence of cationic polymers (Liu, Vesterinen, Genzer, Seppälä, & Rojas,
75 2011; Liu et al., 2010). Moreover, instead of becoming attached to the cellulosic substrate before printing, Pluronics can
76 be directly included in the ink formulation, which is particularly useful for the inkjet printing of proteins (Mujawar, Van
77 Amerongen & Norde, 2015).

78 In light of the aforementioned hypotheses and previous findings, paper sheets were coated using different concentrations
79 of SB, HCS, Pluronics (P127 and F127), precipitated calcium carbonate (PCC), alkyl ketene dimer (AKD) and optical
80 brightening agent (OBA). This study also illustrates the use of a statistical tool to design the coating experiments and to
81 identify the most important factors to be considered for improving the paper printability. A comparison of HCS and SB
82 coatings was also explored, discussing their influence on the whiteness of paper, given that the interaction between
83 cationic polymers and OBAs, generally anionic, has been pointed out as a major cause of fluorescence quenching (Shi et
84 al., 2012). All in all, this is the first work assessing the combination of cationic starches and Pluronics in paper coating,
85 and it does so with an in-depth evaluation of their effects on optical, surface and printing properties.

86

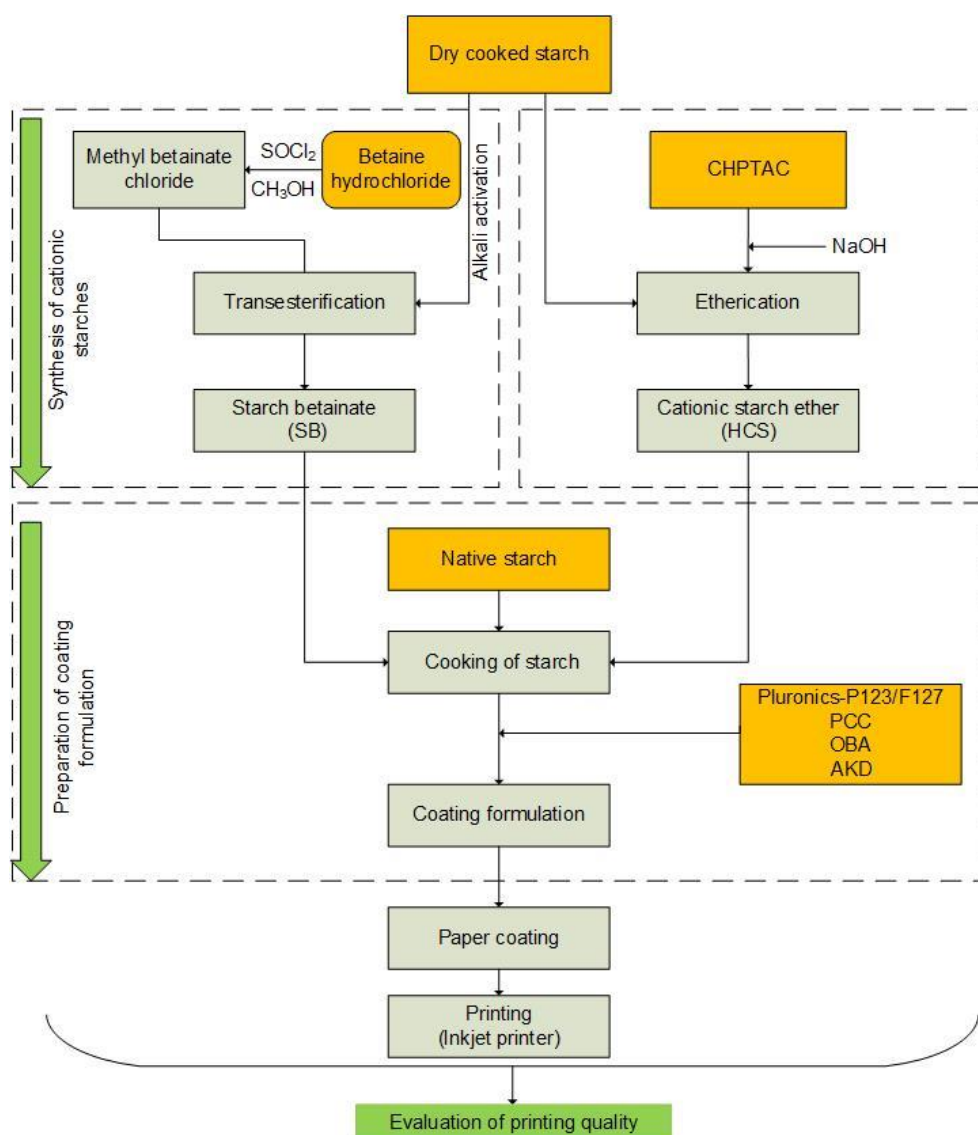
87 **Materials and Methods**

88 **Materials**

89 Native corn starch (NS), α -amylase (in standard buffer solution, pH 5.8), PCC, OBA and AKD were of industrial origin.
90 3-Chloro-2-hydroxypropyltrimethyl ammonium chloride (CHPTAC), Pluronics® P123 (MW $\sim 5750 \text{ g mol}^{-1}$, PEO ~ 30
91 % wt. and CMC of 0.313 mM at 20 °C) (Alexandridis, Holzwarthf, & Hatton, 1994) and Pluronics® F127 (MW
92 $\sim 12600 \text{ g mol}^{-1}$, PEO-70 % wt. and CMC of 0.56 mM at 25 °C) (Thapa, Cazzador, Grønlien, & Tønnesen, 2020) were
93 purchased from Sigma-Aldrich. Betaine hydrochloride (99%) was purchased from Alfa Aesar and used as-is for
94 transesterification. All solvents were purified or dried prior to use the standard procedures. Other commercially available
95 compounds were used without further purification.

96 Figure 1 schematizes the methods, highlighting the aforementioned materials and displaying all the steps taken towards
97 coated and inkjet-printed paper sheets.

98



99

100 Figure 1 Outline of the experimental procedure.

101

102 Synthesis of HCS and SB

103 Native starch was mildly hydrolyzed with α -amylase ($0.45 \mu\text{L g}^{-1}$ of starch), under continuous stirring, at 80°C for 5
 104 min. The temperature was raised up to $90\text{--}95^\circ\text{C}$ for 15 min. Then, the starch solution was cooled down and absolute
 105 ethanol was added to precipitate the polysaccharide, hereinafter referred to as “cooked starch”. Cooked starch was then
 106 vacuum filtered, dried and stored in an oven at 50°C . This pretreatment is common to the synthesis of both HCS and
 107 SB.

108 HCS was synthesized as described elsewhere (Haack, Heinze, Oelmeyer, & Kulicke, 2002). Briefly, 10 g of cooked or
 109 native starch was converted into HCS using 33.5 mL of CHPTAC (60% wt.) and 5.9 g of NaOH. The reaction was
 110 carried out for 24 h at 70°C in 100 ml of distilled water. The reaction mixture was then neutralized with a 0.1% HCl
 111 solution.

112 Starch betainate (SB) was synthesized, as described in a previous paper (Sharma, Aguado, Murtinho, Valente, &
113 Ferreira, 2021), through the transesterification of starch with methyl betainate (MeBetCl) in polar aprotic solvents. 24 g
114 of betaine hydrochloride was first esterified to synthesize MeBetCl using 11.3 mL of thionyl chloride and 75 mL of
115 methanol, under reflux, for 4 h at 70 °C. MeBetCl was recovered through evaporation of methanol followed by
116 trituration in diethyl ether and, finally, the crude product was dried under high vacuum. Then, 10 g of starch were
117 converted into SB using 20.8 g of MeBetCl in *N,N*-dimethylformamide (DMF), 100 mL. Prior to transesterification,
118 cooked starch was pre-activated in NaOH/ethanol. The reaction was carried out for 24 h at 70 °C.
119 HCS and SB were precipitated by adding ethanol (alcohol/water > 10, v/v), vacuum filtered and washed with absolute
120 ethanol, followed by drying at 50 °C.
121

122 **Characterization of synthesized cationic starches**

123 Attenuated Total Reflectance-Fourier Transform Infrared (ATR-FTIR) spectroscopy, ¹H-nuclear magnetic resonance
124 (¹H-NMR) spectroscopy and viscometry analysis were performed to characterize the synthesized cationic starches.
125 ATR-FTIR spectra were recorded by using an Agilent Cary 630 spectrometer, from 750 to 3000 cm⁻¹, at a resolution of
126 4 cm⁻¹ and 64 scans per sample. NMR spectra were obtained from a Bruker Biospin GmbH spectrometer, at 400 MHz,
127 using D₂O as solvent. The degree of substitution was calculated from the area of the singlet assigned to the methyl
128 protons of the quaternary ammonium group. The reliability of this result was confirmed by measuring the nitrogen
129 percentage of samples on a Fisons Instruments EA 1108 CHNS-O elemental analyzer.
130

131 **Paper coating**

132 NS was used as a common component for preparing all formulations in this work. For that, NS was cooked as described
133 earlier, and then cooled down to 50 °C instead of precipitated. An industrial calendered uncoated paper (base paper, BP),
134 produced from bleached eucalyptus kraft pulp with a basis weight of ~ 78 gm⁻², was used as substrate for performing
135 surface coating.

136 Coating of BP was performed using a Mathis laboratory coater, with a pre-drying infrared system coupled to the
137 applicator bar (SVA-IR-B). An applicator roll with the diameter of 0.13 mm, in conjunction with a velocity of 6 m min⁻¹
138 and intermediate load at both sides, was used to achieve 1.5 to 3 g m⁻² per side, on the basis of dry coating weight.
139 Coated paper sheets were air dried at room temperature.

140 Besides NS, BP sheets were coated with SB, HCS, P123, F127, PCC, and combinations thereof. Coatings were
141 performed using 8%, 16% and 24% of total solids coating weight of each of these components, and several combinations
142 of them were tested at said concentrations. The coating compositions resulting from individual components (with NS)
143 and combinations thereof are shown in Table 1 and 2, respectively.

144 The surface weight gain was calculated by the difference between basis weights (ISO standard 536:1995) of the air-dried
145 coated paper sheet and the respective BP sheet. Before characterization, all coated papers were kept at controlled
146 temperature (23 °C ± 1) and humidity (RH 50% ± 2). For each run, three numbers for paper sheets were coated and
147 characterized for evaluating the printing quality.

148

149

150 Table 1. Composition of coating components expressed as %w/w, on the basis of dry coating weight.

Ingredients	Coating formulations													
	HCS/SB				P123			F127			PCC			Reference
HCS/SB	8	16	24	16										
P123					8	16	24							
F127								8	16	24				
PCC											8	16	24	
OBA	6	6	6		6	6	6	6	6	6	6	6	6	6
AKD	0.4	0.4	0.4	0.4	0.4	0.4	0.4	0.4	0.4	0.4	0.4	0.4	0.4	0.4
NS	85.6	77.6	69.6	83.6	85.6	77.6	69.6	85.6	77.6	69.6	85.6	77.6	69.6	93.6

151

152 Table 2. Composition of coating components for the interaction study, expressed as %w/w, on the basis of dry coating weight.
153

Ingredients	Coating formulations										
	HCS/SB +P123					HCS/SB +P123+PCC					Reference
HCS/SB	16	16	16	16	16	16	16	16	16	16	
P123	8	16	24	16	8	16	24	16			
PCC					16	16	16	16			
OBA	6	6	6		6	6	6				6
AKD	0.4	0.4	0.4	0.4	0.4	0.4	0.4	0.4	0.4	0.4	0.4
NS	69.6	61.5	53.6	67.6	53.6	43.6	37.6	51.6			93.6 99.6

154

155 **Paper properties**156 **Surface and optical properties**157 Surface and cross-section micrographs of coated papers were obtained by means of a field emission scanning electron
158 microscope (FE-SEM), Merlin (Carl Zeiss AG), including a Gemini II column and a backscattered electron detector.159 Bendtsen roughness (ISO 5636-3, 8791-2) and Gurley air permeability (ISO 5636/5) were also measured for coated
160 papers using appropriate testers from Flank. Whiteness (CIE W D65/10) of coated papers was measured using D65
161 illumination in the Elrepho spectrophotometer. The average value and the standard deviation of four independent
162 measures are reported for CA, Bendtsen roughness, Gurley air permeability and whiteness. This last property was
163 related to the performance of OBA, as fluorescence emission spectra of solutions containing OBA were recorded by
164 means of a FluoroMax 4 spectrofluorometer from Horiba.165 **Resistance to water**

166

167 The surface hydrophilicity for SB-coated papers was evaluated by contact angle goniometry. The static water contact
168 angle (WCA) was measured in an OCA 20 goniometer (Dataphysics, Germany) using the sessile drop method. A droplet
169 of deionized water (10 μ L) was automatically poured onto the coated paper surface. After settling, the formed angle was
170 measured by fitting the Young-Laplace equation to the drop profile.

171 **Viscosity and thermal degradation behavior**

172 The kinematic viscosity was determined using a size 100 Cannon-Fenske viscometer in a thermostatic bath (TAMSON
173 TV 2000) set at 40 °C. Measurements followed the ISO 3105 standard. Polymer solutions were prepared with a
174 concentration of 5 mg cm⁻³ in 1M NaOH/H₂O (for HCS) and DMSO (for SB).

175 The thermogravimetric analysis (TGA) was carried out on a thermo-microbalance TG 209 F3 Tarsus, from Netzsch
176 Instruments. Samples were heated from 40 °C to 600 °C, under a flow of nitrogen (20 mL min⁻¹), with a heating rate of
177 10 °C min⁻¹. TGA was performed for filter paper coated with P123, F127 and SB. A filter paper was cut into pieces
178 (5cm × 2 cm) and Pluronic P123/F127 were absorbed in this cellulosic substrate. This was carried out with a 10%
179 Pluronic aqueous solution and a LayerBuilder dip coater from KSV. Cellulose substrates were dipped into the solution
180 for 3 min, pulled out and air-dried. The same procedure was followed for 10% SB and 10% P123/F127 + 10% SB
181 aqueous solutions.

182

183 **Printing quality**

184 Samples for measuring the printing quality were prepared as reported elsewhere (Lourenço, Gamelas, Sarmiento, &
185 Ferreira, 2020). Briefly, the coated papers were printed using HP Officejet Pro 6230 inkjet printer, having cyan,
186 magenta, yellow, and black color ink cartridges. The printed sheets were air dried for 4 h under controlled conditions of
187 temperature and humidity.

188 **Gamut area and gamut volume**

189 The GA is the area of the hexagon resulting from the a* and b* coordinates of six printed colors (red, green, blue, cyan,
190 magenta, and yellow), where a* axis represents the color from green to red and axis b* represents the color from blue to
191 yellow. It was determined by measuring the values of CIE L*a*b* coordinates for six color spots, including three base
192 colors (cyan, magenta and yellow) and other three complimentary colors (red, green and blue). For that, the “X-Rite Eye
193 One XTreme UV Cut” spectrophotometer was placed on each printed color spot, activating the UV light (D50, 2°). The
194 readings were taken in the sequence of red, green, blue, cyan, magenta, and yellow color spots. Additionally, CIE
195 L*a*b* values for black and white colors were measured to estimate the gamut volume (GV) of printed paper sheets.

196 **Optical density, print-through, bleed, and circularity**

197 In order to evaluate OD and PT, the QEA PIAS-II spectrophotometer was used with a low resolution optical module
198 (33µm/pixel with visual area of 21.3mm × 16mm), along with the software PIAS II, based on ISO 13660 quality
199 standards, for processing the images. The PT of a printed paper requires the measurement of L*a*b* values on the
200 opposite side, in contrast with the non-printed area of the same paper sheet. The transmitted light intensity from a
201 specific area of each color (black, white, cyan, magenta, and yellow) was measured using QEA PIAS-II, and thus PT
202 and OD were calculated from the following equations:

$$203 \quad \text{Optical density} = \text{Log}_{10}(\text{Insident light}/\text{Transmitted light}) \quad \text{Equation 1}$$

204

205
$$Print\ through = \sqrt{(L_p^* - L_u^*)^2 + (a_p^* - a_u^*)^2 + (b_p^* - b_u^*)^2}$$
 Equation 2

206 where L^* , a^* , b^* are the CIE chromatic coordinates, and the subscripts u and p refer to areas of unprinted and back of
207 the printed black spot, respectively.

208 The other printing properties, namely ITCB and circularity (black), were also evaluated by means of QEA PIAS-II with
209 high resolution module (5 $\mu\text{m}/\text{pixel}$ with 3.2mm \times 2.4mm). This was used to measure the raggedness, which can be
210 defined as the geometric distortion of the line and dots, given by the standard deviation of the residue from the lines and
211 dots adjusted to their ideal limit. The higher the raggedness, the worse the ITCB and circularity.

212 **Statistical analysis**

213 In order to observe the interactions between coating components and their impact on the printing quality of coated
214 papers, TIBCO's Statistica software was used as a statistical tool for the design of experiments and data analysis. In this
215 study, four continuous factors, namely HCS, P123, PCC and OBA, were selected, each at two levels (0 and 16%), and a
216 full factorial design with two center points was chosen to design the coating experiments. A total number of 16 runs
217 were performed to evaluate the effect of these factors and their binary or ternary interactions on the printing quality,
218 namely: GA; OD for cyan, magenta, yellow, and black; PT; inter-color bleed (ITCB), and circularity for black color in
219 the responses.

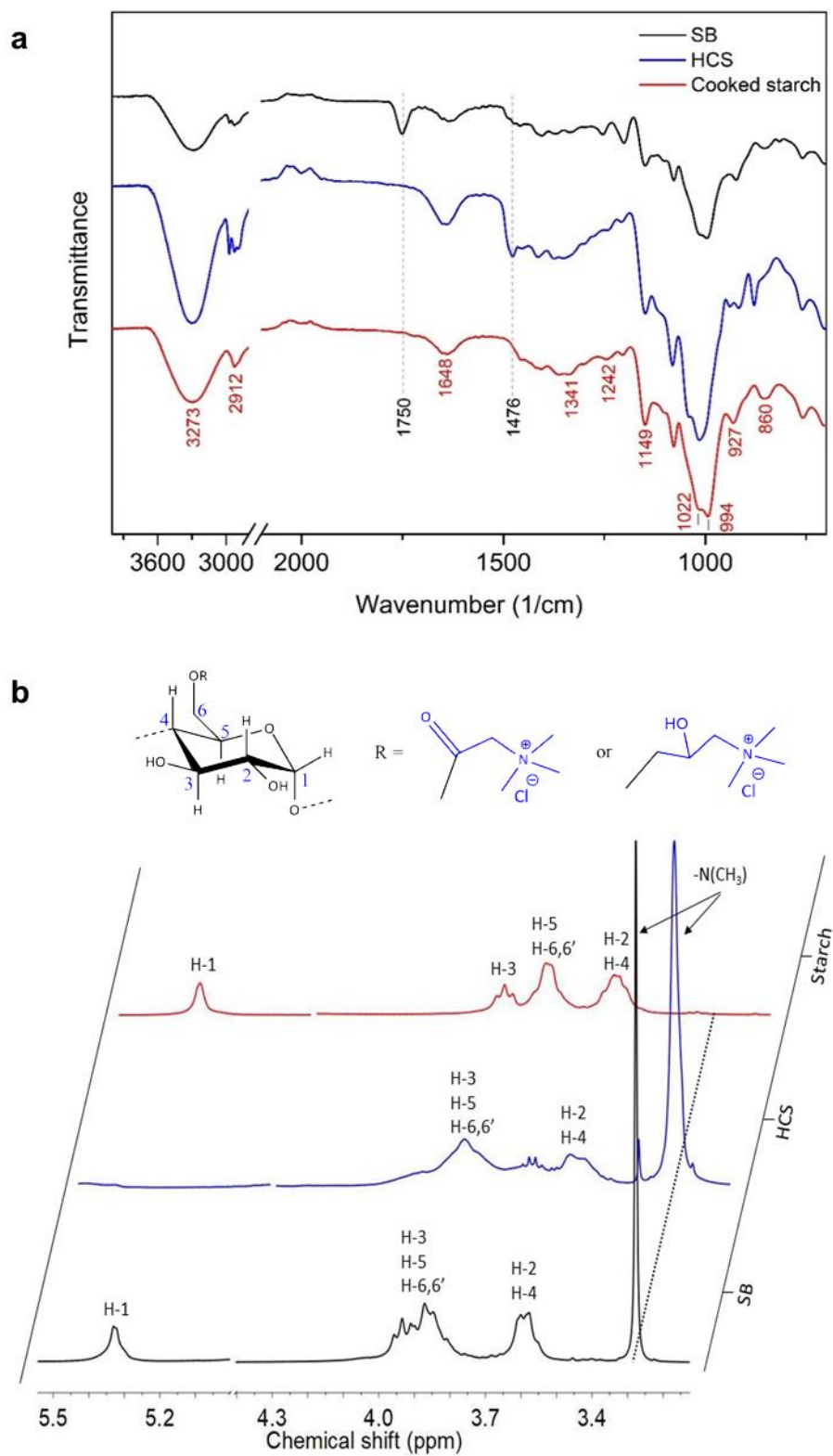
220

221 **Results and discussion**

222 **Synthesis of SB and HCS**

223 Figure 2a presents the ATR-FTIR spectra for synthesized cationic starches from etherification and transesterification,
224 using respectively CHPTAC and betaine hydrochloride, in comparison to the NS spectrum. The absorption peaks at
225 3300 cm^{-1} , 2912 cm^{-1} , 1648 cm^{-1} can be assigned to the $-\text{OH}$, $-\text{CH}_2$ stretching vibrations, and H_2O bending vibration
226 due to water sorption, respectively. Additionally, peaks at 994 cm^{-1} can be attributed to the ether bonds and the
227 absorption band at 897 cm^{-1} can be assigned to C1-H bending in starch. Compared to cooked starch, a new prominent
228 peak at 1473 cm^{-1} can be observed due to the quaternary ammonium group attached to the anhydroglucose unit (AGU)
229 (Hebeish, Higazy, El-Shafei, & Sharaf, 2010; Wang & Cheng, 2009). Furthermore, the absorption band at 1750 cm^{-1} is
230 assigned to the ester bond in SB.

231 Figure 2b shows the $^1\text{H-NMR}$ spectra for HCS and SB, compared to the spectrum of cooked starch. The singlet at 3.28
232 ppm is assigned to the nine hydrogens of methyl groups of the quaternary ammonium. The resonances from 3.5 to 4 ppm
233 represent the hydrogens attached to carbons 2, 4, 5, 6 (H-6 and H-6'), and 3 of AGU, typically in that order. The doublet
234 for the H-1(α) anomeric proton lies downfield (5.35 ppm). There was a certain shift upfield and broadening of all signals
235 upon cationization. No impurities were detected in SB, but the HCS spectrum displayed a singlet at 3.33 ppm and a
236 quadruplet at 3.65 ppm, none of which belong to the canonical structure of cationic starches. The former could be due to
237 quaternary ammonium groups arising from substitution on hydroxypropyl chains, instead of the hydroxyl groups of
238 AGU.



240

241

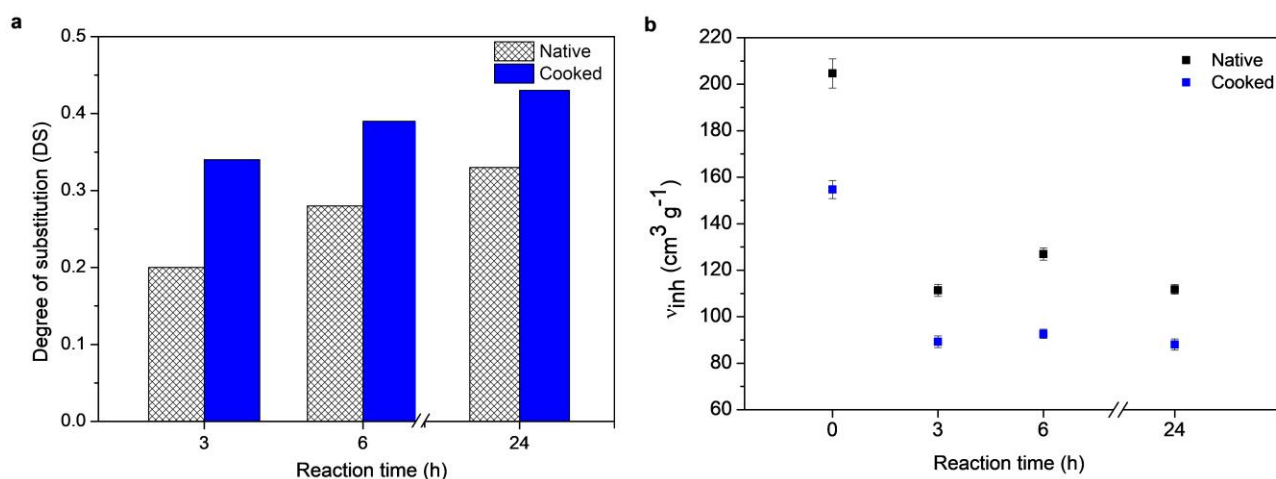
242

243

Figure 2 ATR-FTIR (a) and ¹H-NMR (b) spectra for cationic starch ether and starch betainate, compared to cooked starch.

244 An important hypothesis regarding the reaction is that enzymatic cooking improves its efficiency. Figure 3a shows the
 245 effect of cooking and reaction time on the DS of the synthesized HCS. It can be observed that the DS increases from
 246 0.20 to 0.33 and from 0.34 to 0.43 with the increase in the reaction time from 3 to 24 h, when native and cooked starches
 247 were used as raw materials for the etherification reactions, respectively. This is likely due to the formation of more
 248 porous starch granules, which facilitates the access of the reagent to hydroxyl groups (Huber & BeMiller, 2001). It was
 249 also observed that the cooking of starch enables the homogeneous dispersion of starch granules in the solvent by
 250 increasing the solubility and decreasing its viscosity, as seen in Figure 3b (Gao, Luo, Fu, Luo, & Peng, 2012).

251 Undoubtedly, due to the cleavage of 1–4 α -D-glucopyranosyl linkages of amylose and amylopectin, the inherent
 252 viscosity decreases with the enzymatic pre-treatment, from $199.4 \text{ cm}^3 \text{ g}^{-1}$ (NS) to $151.8 \text{ cm}^3 \text{ g}^{-1}$ (cooked starch). The
 253 viscosity was further reduced by 43–45% when using them in etherification. Likewise, the hydrolysis of starch
 254 molecules in highly alkaline media and at high temperature is evidenced by a loss of viscosity after functionalization.
 255 Nonetheless, after reaction times beyond 3 h, further hydrolysis is either negligible or compensated by the effects of
 256 cationization on polymer-solvent interactions.



257
 258 Figure 3 Effect of reaction time and enzymatic cooking on degree of substitution (A) and inherent viscosity (B) of HCS.

259 Like etherification, the increase in DS and decreasing in viscosity were also observed in the synthesis of SB. However,
 260 DS increased much more abruptly, from 0.01 to 0.33, when using NS and cooked starch in the transesterification
 261 reaction, respectively, proving the poor reaction efficiency with NS. Given that the inherent viscosity decreased by
 262 ~73%, starch faced higher depolymerization during functionalization, mostly due to the previous alkalization of starch at
 263 high temperature.
 264

265

266 Properties of coated sheets

267

268

269 **Paper printing properties**

270 Both native starch and CS require cooking before adding other coating components to prepare a uniform coating
271 solution. It should be noted that the other coating components (PCC, Pluronics, OBA and AKD) were always added
272 after cooling down the starch solution to 50 °C. It should be stressed that the P123 and F127 have critical micelle
273 concentrations of 0.313 mM (20°C) and 0.56 mM (25°C), respectively. These values are lower than the amount of
274 Pluronics used in the experiments reported here; additionally, the critical micelle temperatures of these surfactants are
275 well below 50 °C which also support that Pluronics are in the micelle form (He & Alexandridis, 2018).

276 In order to prepare the coating formulations, corn native starch was used as host component and cooked using α -
277 amylase enzyme in aqueous medium at 80 °C, for 5 min. CS was then added and cooked together with native starch at
278 90-95 °C for 15 min. The starch solution was cooled down for 15 min.

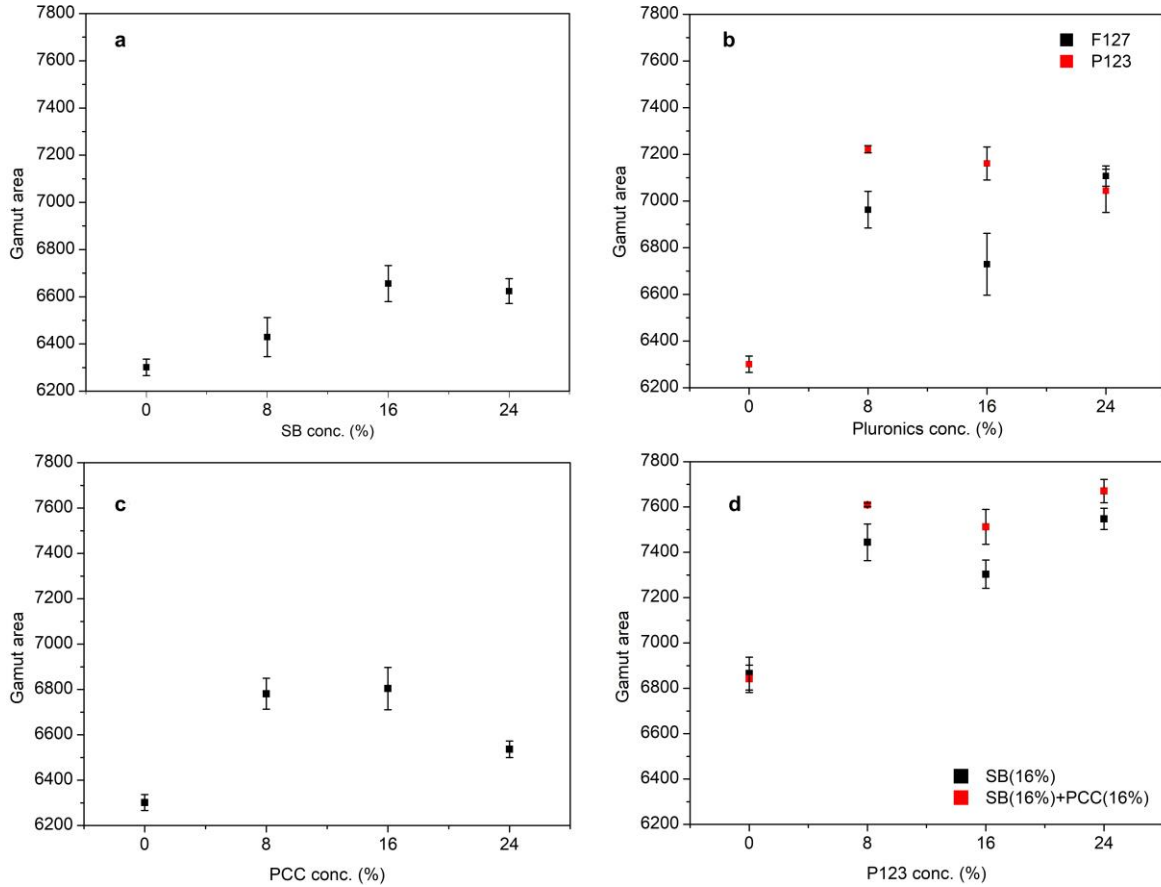
279

280 **Gamut area**

281 It was observed that the GA, presented in Figure 3a, increased by 8.6%, 9%, and 12.5% using 8%, 16% and 24% dry
282 solids content of SB, respectively, compared to NS coating. Plausibly, the high DS led to higher deposition of SB on the
283 paper surface, resulting into improved GA (Niegelhell et al., 2018).

284 Besides charge density, addition of SB slightly increased the hydrophobicity of the paper surface and smoothness; both
285 also contributed to improve GA (Gigac, Stankovska, & Pazitny, 2016) (Gigac, Stankovska, et al., 2016). Table 4 can be
286 referred to for the Bendtsen roughness, and contact angle values for SB coated papers.

287 Similarly to GA, GV, which considers the color luminance L, besides a and b, also increased with increasing SB
288 concentration. The maximum increase was observed as 16.4% using 24% of SB, compared to NS coating (refer Table
289 4).



290
291 Figure 3 Effect of different concentrations of SB (a), Pluronic (b), PCC (c), and their combinations (d) on GA.

292
293 Table 3 Properties of coated papers using different concentrations of SB, Pluronic (P123 and F127), and their
294 combination in coating formulations.

	Conc. (%)	Roughness (mL/min)	Gurley (mL/min)	Contact angle (°)	Whiteness	Gamut volume / 10 ³	Weight gain (g/m ²)
Reference (NS)		329 ± 13	318 ± 7	72 ± 1	162.8 ± 1.3	132 ± 1	1.8 ± 0.3
SB	8	324 ± 14	379 ± 14	75 ± 2	162.3 ± 0.5	146 ± 1	2.5 ± 0.2
	16	311 ± 7	397 ± 4	77 ± 2	164.5 ± 0.3	151 ± 1	1.9 ± 0.2
	24	376 ± 9	420 ± 16	79 ± 1	164.1 ± 0.7	153 ± 1	2.3 ± 0.3
P123	8	368 ± 9	407 ± 6	50 ± 3	165.1 ± 0.2	153.3 ± 0.4	2.9 ± 0.2
	16	379 ± 30	381 ± 5	43 ± 2	165.6 ± 0.2	152 ± 2	2.9 ± 0.1
	24	357 ± 9	354 ± 9	47 ± 1	165.8 ± 0.4	150 ± 2	3.0 ± 0.2
F127	8	378 ± 38	356 ± 5	63 ± 3	163.6 ± 0.6	145 ± 2	2.4 ± 0.2
	16	363 ± 28	325 ± 50	57 ± 1	163.4 ± 0.4	141 ± 3	2.7 ± 0.1
	24	329 ± 18	444 ± 13	53 ± 2	162.2 ± 0.7	150 ± 1	2.7 ± 0.2
PCC	8	414 ± 37	347 ± 5	75 ± 2	160.9 ± 0.3	149 ± 1	2.5 ± 0.3
	16	370 ± 15	381 ± 11	83 ± 2	161.3 ± 0.1	146 ± 1	2.5 ± 0.2
	24	365 ± 5	367 ± 2	80 ± 2	162.5 ± 1.1	143 ± 1	2.7 ± 0.1
P123 (with SB)	8	375 ± 22	376 ± 21	51 ± 3	164.9 ± 1.7	162 ± 3	2.4 ± 0.1
	16	383 ± 36	321 ± 9	48 ± 2	165.4 ± 0.8	161 ± 2	2.8
	24	368 ± 13	374 ± 13	40 ± 3	163.6 ± 0.5	164 ± 2	2.7 ± 0.1

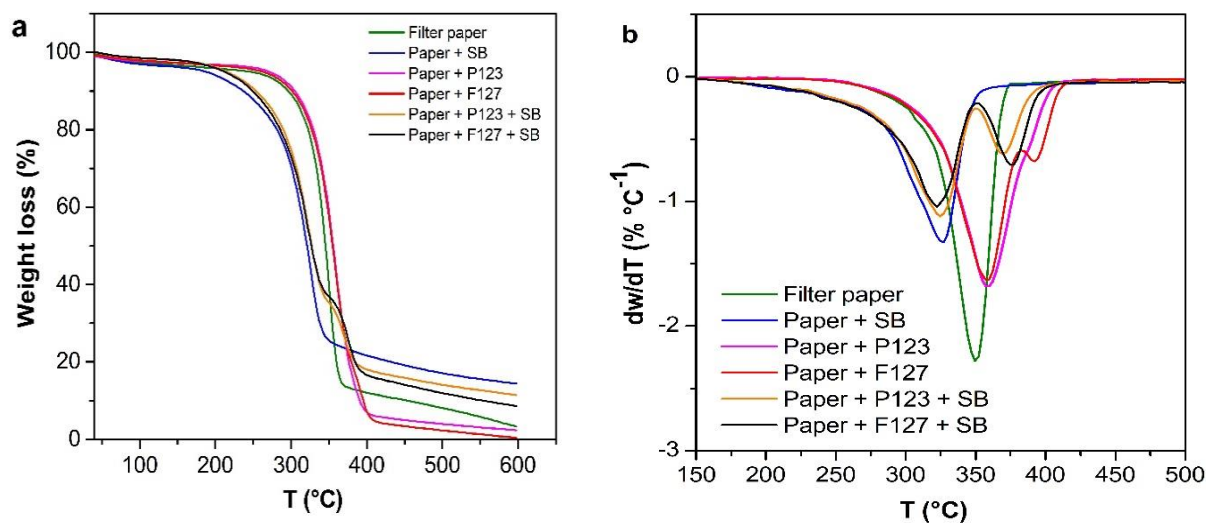
295

296 In Figure 3b, the GA for different concentrations of Pluronics P123 and F127 is presented. GA is improved by 14.6%
297 using 8% of P123 in the coating solution; however, the GA is further reduced by increasing the P123 concentration from
298 8% up to 24%. For F127, the 8% addition improves the GA by 10.5%, but further increase in the concentration of F127,
299 from 8 up to 16%, reduces the GA as well. However, the use of 24% of F127 showed almost equal GA increase as 24%
300 of P123, 11.8% and 12.8%, respectively. The increase of GA can be explained by the amphiphilic nature of Pluronics,
301 which facilitates the strong adsorption of these components on cellulosic surfaces (Liu et al., 2010). Additionally,
302 Pluronics form inclusive complexes with starches, leading to the formation of self-supporting flocs in the coating
303 formulation, and enhancing the dispersion of other coating components (Petkova-Olsson et al., 2017; Petkova-Olsson,
304 Ullsten, & Järnström, 2016). Remarkably, the lowest amount of P123 and F127 (8%) was found to be more favorable to
305 improve GA. This area was also improved by ~7.9% in the presence of PCC at a concentration of 8% or 16% (Figure
306 3c), which is related to the gain in hydrophobicity of the paper surface. However, roughness increased with the presence
307 of PCC and GA was further decreased by 3.7% with a large content of PCC (24%) in the coating formulation.

308 The effect of P123 coatings in combination with SB (16%) and SB (16%)/PCC (16%) is displayed in Figure 3d. It is
309 observed that GA increases by 8.5-9% using P123 or a mixture of P123 and PCC. It was further improved significantly
310 by 16-20% and 19-22% with the presence of SB/P123 and SB/P123/PCC, respectively. This increase in GA can be
311 explained by the sorption of Pluronics on the cellulosic surface, which increases in combination with a highly cationic
312 polymer (Liu et al., 2011, 2010). Moreover, formation of amylose-Pluronics inclusion complexes may also facilitates the
313 immobilization of the ink pigments on the coated paper surface, improving GA.

314 TGA contributes to understand the adsorption of Pluronics in the presence of a cationic polymer. Figure 4 (a) and 4 (b)
315 represent the TGA and DTG curves of dip-coated paper samples, respectively. It can be seen that the major
316 decomposition areas can be divided into three zones, 275 to 350 °C, 300 to 350 °C and 325 to 400 °C for SB coatings,
317 filter papers and Pluronics coatings, respectively. However, an increase in the major decomposition area of both
318 Pluronics was observed when filter papers were coated with the presence of SB (+Pluronics), which can be attributed to
319 an increased adsorption of Pluronics in the presence of SB.

320



321

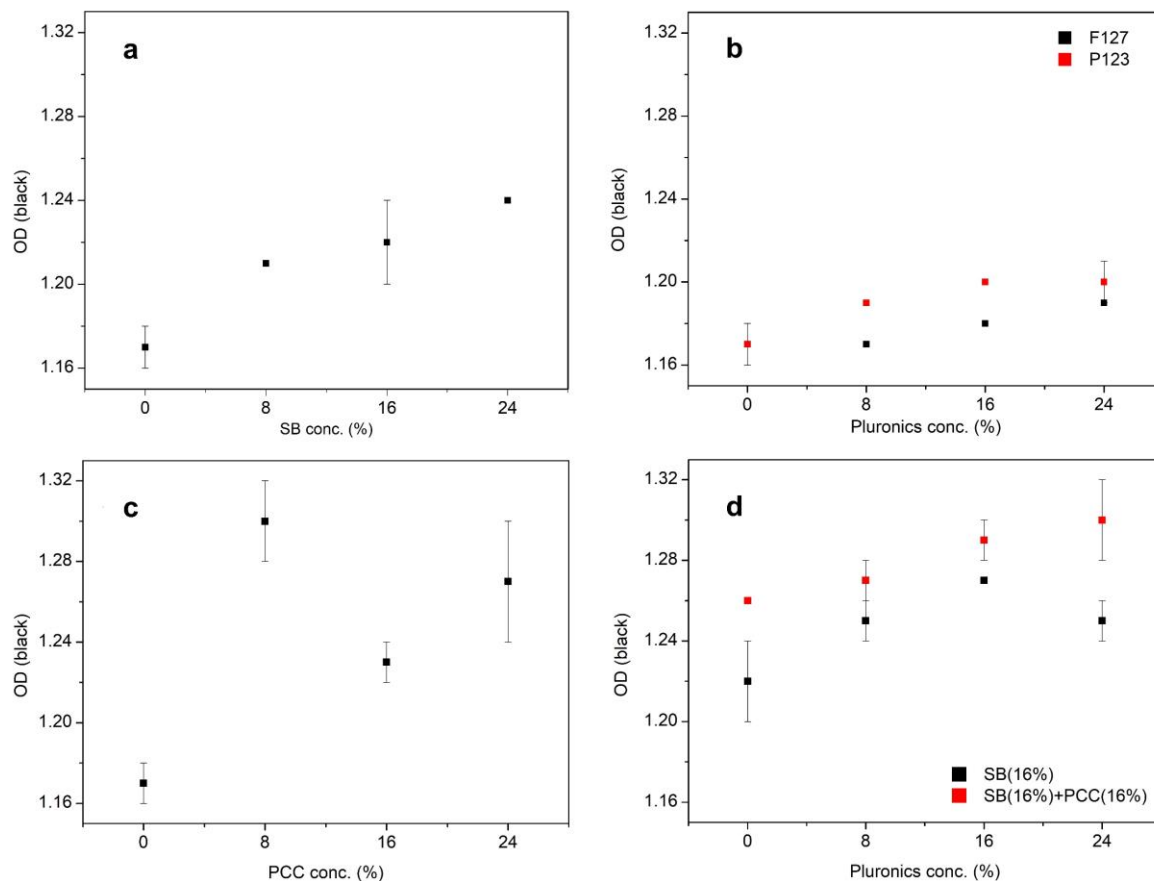
322 Figure 4 TGA (a) and DTG (b) curves for filter paper, paper + SB, paper + P123, paper + F127, paper + P123 + SB and
 323 paper + F127 + SB.

324

325 **Optical density**

326 OD is an important parameter to evaluate the depth of the color tone in the printed papers, which clearly affects the
 327 perceived saturation of a color (Hu, Fu, Chu, & Lin, 2017). Figure 5 represents the OD of the black color with increasing
 328 concentration of SB (A), Pluronic (B), PCC (C) and SB/P123/PCC (D). Figure 5c shows the effect of PCC
 329 concentration on OD. OD for PCC coating correlates with the Gurley permeability, attaining deeper tones as the sheet
 330 became more resistant to air flow (Kasmani, Mahdavi, Alizadeh, Nemati, & Samariha, 2013). The highest improvement
 331 was observed at 8% of PCC. Likewise, OD followed the same trends as GA, and thus it increased with increasing
 332 concentration of SB and P123/F127. Above all, Figure 5d shows that the highest increase in OD was achieved with the
 333 combination of SB-P123-PCC in the coating formulation.

334



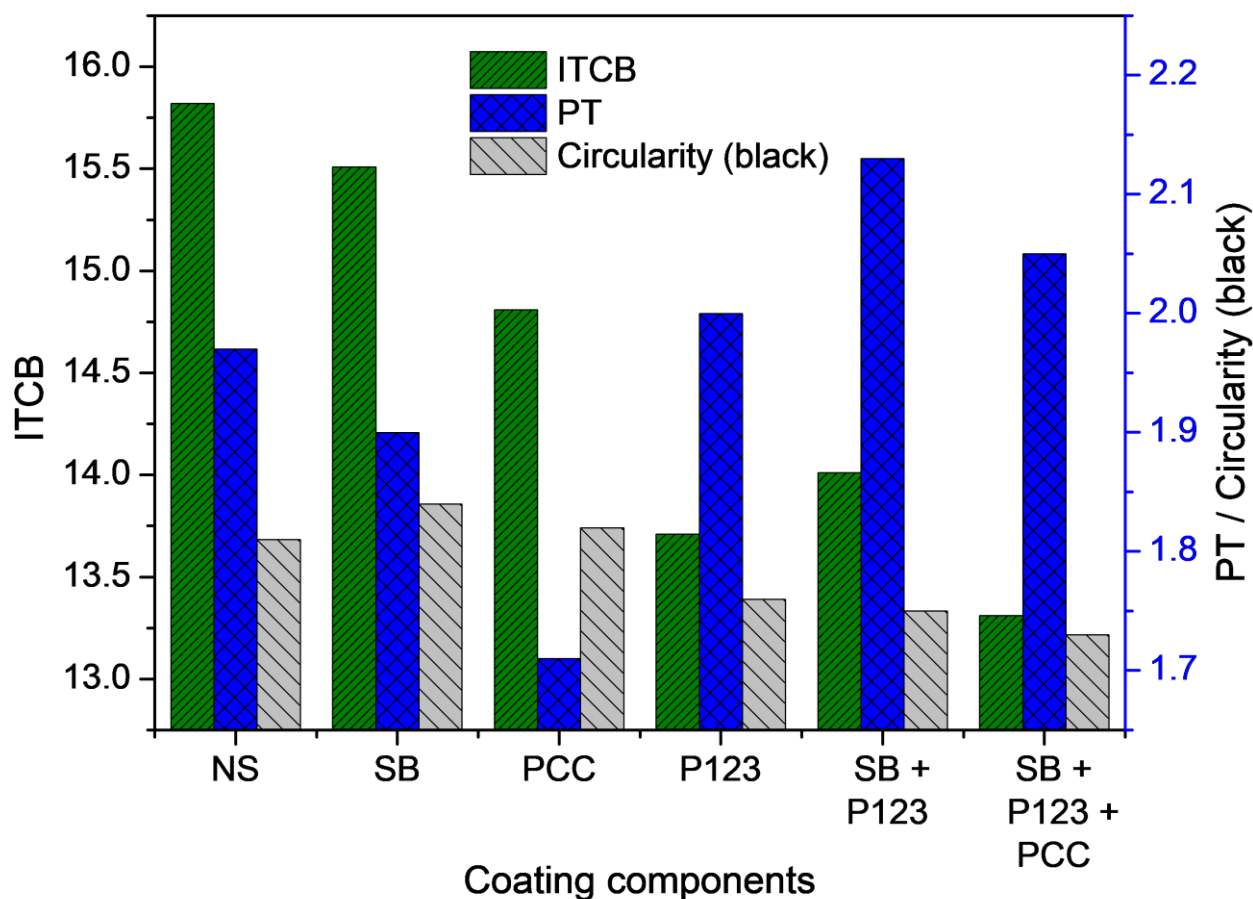
335

336 Figure 5 Effect of different concentrations of SB (a), Pluronics (b), PCC (c) and their combinations (d) on OD (0%:
 337 reference coating using NS).

338

339 **Inter-color bleed (ITCB), print-through (PT) and circularity for black color**

340 Figure 6 presents the ITCB, PT and circularity (black dots) of SB, PCC, P123, SB/P123 and SB/P123/PCC coated
 341 papers. Similarly to GA, ITCB was also improved (*i.e.*, reduced) upon the addition of these components. The highest
 342 decrease in ITCB, 15.9%, was observed with SB/P123/PCC coatings. Unlike GA and ITCB, PT of SB/P123 or
 343 SB/P123/PCC coated paper showed a higher PT at the concentrations used in this work, due to decrease in viscosity of
 344 the coating formulation, letting the formulation go deeper into the cellulose matrix, which increased the see-through of
 345 ink from the other (non-coated) side of the paper. The presence of PCC on the cellulosic surface provided a better
 346 improvement in the PT compared to SB or P123 coated papers. Circularity of black dots generally correlates with the
 347 ITCB, improving with the formulation containing SB and P123, due to better fixation of ink particles onto the surface.



348

349 Figure 6 Effect of different coating components on ITCB, PT and circularity of black color.

350

351 **Whiteness and fluorescence quenching**

352 Whiteness, positively correlated with ISO brightness, represents a paper's ability to equally reflect a balance of all
 353 wavelength of light across the visible spectrum (Hu et al., 2017). The addition of OBA on the paper surface is a cost-
 354 effective solution in papermaking to increase the whiteness of printing and writing papers (Shi et al., 2012). Therefore,
 355 the interaction between OBA and the other coating components is important. From Table 4, it can be noted that the
 356 presence of OBA improved the whiteness of the coated paper but the presence of HCS quenched this agent, resulting in
 357 lower whiteness (Figure S1, Supplementary Information). It is also worth mentioning that the presence of P123 and PCC
 358 did not show any further improvement in the whiteness.

359

360 Table 4 Study of interactions among factors. Percentages are related to the total solids content (on the basis of dry
 361 weight) of coating formulations.

HCS (%)	P123 (%)	PCC (%)	OBA (%)	GA	OD (cyan)	OD (Magenta)	OD (yellow)	OD (black)	PT	ITCB	Circularity (Black)	Whiteness
0	0	0	0	6512	0.76	0.87	1.31	1.23	1.6	15.5	1.95	146
0	0	0	6	6301	0.74	0.84	1.31	1.17	1.97	15.8	1.81	162
0	0	16	0	6596	0.76	0.88	1.33	1.20	1.56	15.4	1.98	146

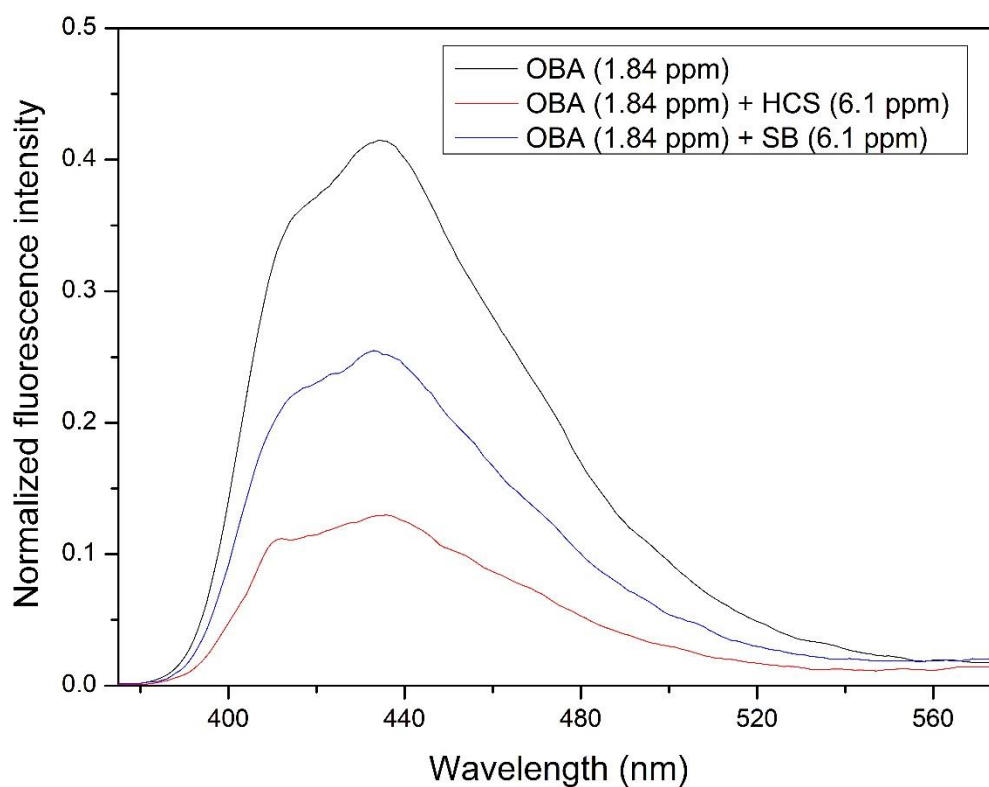
0	0	16	6	7074	0.80	0.91	1.36	1.21	1.76	14.4	1.81	162
0	16	0	0	6758	0.79	0.89	1.33	1.22	1.76	14.5	1.80	146
0	16	0	6	6922	0.80	0.90	1.34	1.20	1.86	13.7	1.76	162
0	16	16	0	7004	0.81	0.90	1.34	1.20	1.80	14.2	1.74	146
0	16	16	6	6802	0.81	0.90	1.33	1.21	1.69	14.0	1.71	163
8	8	8	3	7122	0.82	0.90	1.34	1.19	1.65	13.8	1.80	148
8	8	8	3	7212	0.82	0.91	1.33	1.20	1.69	14.2	1.81	147
16	0	0	0	6610	0.80	0.78	1.33	1.25	1.99	16.0	1.79	144
16	0	0	6	6656	0.74	0.77	1.37	1.24	1.78	16.2	1.79	145
16	0	16	0	6971	0.77	0.88	1.31	1.20	1.82	15.6	1.95	144
16	0	16	6	6739	0.79	0.78	1.31	1.23	1.82	15.6	1.84	146
16	16	0	0	7479	0.83	0.92	1.36	1.22	1.80	12.7	1.83	146
16	16	0	6	7443	0.86	0.85	1.50	1.42	1.66	16.3	1.89	146
16	16	16	0	7427	0.83	0.91	1.35	1.20	1.72	13.9	1.76	145
16	16	16	6	7670	0.85	0.93	1.37	1.22	1.84	13.2	1.71	148

362

363 In comparison to NS coatings, whiteness increased by 11% with the addition of OBA. As aforementioned, HCS (with
364 OBA) reduced the whiteness of coated papers by ~10.85% due to the OBA quenching, irrespective of the presence of
365 any other components. Interestingly, such loss of whiteness was not observed when SB was used instead of the cationic
366 starch ether (Figure S1).

367 To understand the OBA quenching effect in the presence of HCS and SB, fluorescence emission spectra were recorded
368 for solutions containing OBA (1.84 ppm) and either cationic starch (6.1 ppm), so as to keep the same ratio as in coating
369 formulations (6% OBA / 16% CS). Fluorescence quenching was clear in the presence of all cationic starches but, in the
370 case of HCS, the intensity of the emission of blue light (~440 nm) decreased almost by a factor of 4 (Figure 7).

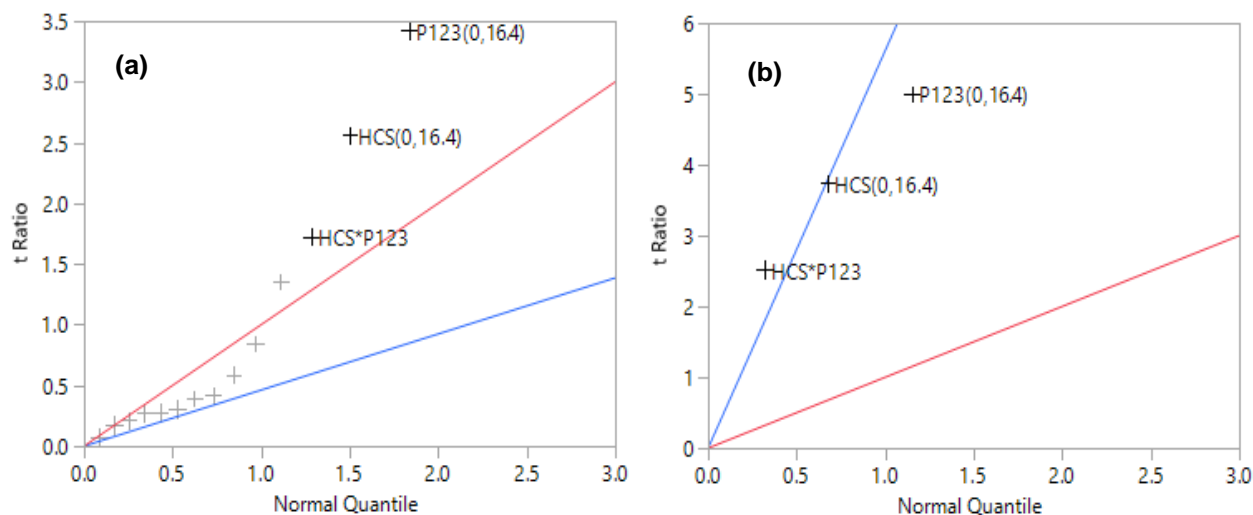
371 Quenching was possibly due to the formation of a non-fluorescent complex, where the sulfonate groups of OBA donate
372 electrons to the quaternary ammonium groups of HCS. Still, the most plausible explanation is the aggregation-caused
373 quenching, where aggregation is promoted by electrostatic interactions. The reason for this is that solutions at higher
374 concentration, such as 9.2 ppm OBA / 24.4 ppm HCS, showed Rayleigh scattering to such extent that no reliable
375 spectrum could be obtained, even though a concentration of 24.4 ppm lies much below the solubility limit of HCS. In
376 other words, there was a phase transition from solution to dispersion when both solutions, each of them displaying
377 negligible light scattering, were mixed. However, regardless of the quenching mechanism, neither this aggregation nor
378 that extent of quenching was observed when using SB/OBA at the same concentrations, supporting the previously
379 described retention of paper whiteness. Given that SB and HCS had the same DS, it may be concluded that the cationic
380 starch ester possesses a key advantage over its ether counterpart. This advantage should, undoubtedly, be further
381 explored.



382
 383 Figure 7 Fluorescence emission spectrum of OBA in presence of HCS and SB. An excitation wavelength of 350 nm was
 384 used to record all spectrum.

385
 386 **Statistical analysis**

387 Figures 8a and 8b show the half-normal plots, as obtained from TIBCO's Statistica software, for all the studied factors.
 388 As indicated in Figure 8a, three major factors are clearly falling off from the red straight line. In other words, P123, HCS
 389 and their interaction (HCS*P123) can be considered as the most significant factors to affect the GA, whereas PCC and
 390 OBA, like their interaction, were found to be insignificant. The model was further optimized through prediction plots
 391 and ANOVA study, and insignificant factors were removed. Figure 8b indicates the half-normal plot of the model,
 392 considering only the significant factors.
 393



394
395 Figure 8 Half-normal plot for gamut area: a) considering all factors; b) considering only significant factors.

396
397 A prediction profile for GA and a complete report of the model is provided in the Supplementary Information. From this
398 statistical study, it can be inferred that the combination of HCS and Pluronic in the coating formulation, together with
399 the presence of PCC and OBA, led to improve the printability of coated papers. The statistical study of these
400 components has shown that, for GA, the incorporation of P123, the presence of HCS and their interaction, have
401 significant effect in the selected range. Regarding the most important variables for the other printing properties, P123
402 has significant effect on OD for cyan/magenta/yellow and on ITCB, whereas HCS impacts OD of black color. The
403 ternary interaction HCS-P123-OBA showed a good impact on PT (not seen with SB-P123-OBA) and the binary
404 interaction P123-PCC affects the circularity of black color. The corresponding half-normal plot, the analysis of variance
405 and the prediction profiles have also been included in the Supplementary Information. All considered, the combination
406 of both HCS and P123, accounting for a total solids content of 16%, has the greatest impact on the overall printing
407 quality.

408

409 Conclusions

410 The effect of an unconventional combination of coating components, highly substituted cationic starch and Pluronic, on
411 the printing quality of office papers was investigated. As a key novelty, cationic starch refers not only to its typical ether
412 form, but also to starch betainate, an ester that has been suggested for bulk addition in sheet forming but not (as far as
413 the authors are concerned) for paper coating. A 24% coating weight of starch betainate increased the gamut area by
414 12.5%, whilst Pluronic P123 and F127 (8% coating weight) attain improvements of 14.6% and 11.8%, respectively.
415 Both cationic starches, ether and ester, showed the same outcome for improving the paper printing properties in presence
416 and absence of Pluronic. Nonetheless, while the ether caused a certain loss of whiteness, as it quenches the fluorescence
417 emission of the optical agent, such loss was not found when starch betainate was used. The ability of starch betainate of
418 keeping the whiteness gain of an anionic brightening agent is a key finding of this work.

419 Remarkably, the statistical analysis indicated that besides the aforementioned individual effects of cationic starch and
420 Pluronic, the binary interaction thereof had a significantly positive influence on the gamut area. Furthermore, the
421 optical density (cyan, magenta, yellow and black), print-through, inter-color bleed and circularity were successfully
422 correlated with the independent variables. It was shown, for instance, that the print-through was significantly affected by
423 the presence of conventional cationic starch, OBA and Pluronic P123.

424

425 **Declarations**

426 **Funding**

427 This work was carried out under the Project inactus -innovative products and technologies from eucalyptus, Project N.º
428 21874 funded by Portugal 2020 through European Regional Development Fund (ERDF) in the frame of COMPETE
429 2020 nº246/AXIS II/2017. Authors would like to thank the Coimbra Chemical Centre, which is supported by the
430 Fundação para a Ciência e a Tecnologia (FCT), through the projects UID/QUI/00313/2020 and COMPETE. Authors
431 would also like to thank the CIEPQPF - Strategic Research Centre Project UIDB/00102/2020, funded by the Fundação
432 para a Ciência e Tecnologia (FCT). M.S. acknowledges the PhD grant BDE 03|POCI-01-0247-FEDER-021874. R.A.
433 acknowledges the post-doc grant BPD 02|POCI-01-0247-FEDER-021874.

434 **Conflicts of interest/Competing interests**

435 The authors declare that there is no conflict of interest and that they do not have competing interests.

436 **Availability of data and material**

437 All data are displayed in the article and its electronic supplementary information.

438 **Code availability**

439 Not applicable.

440 **Authors' contributions**

441 All authors made substantial contributions to the conception of the work, the acquisition and interpretation of data, and
442 writing. All authors approve the manuscript. All authors agree to be accountable for all aspects of the work in ensuring
443 that questions related to the accuracy or integrity of any part of the work are appropriately investigated and resolved.

444 **Ethics approval**

445 Not applicable. No studies involving humans and/or animals.

446 **Consent to participate**

447 Not applicable. No studies involving humans and/or animals.

448 **Consent for publication**

449 Not applicable. No studies involving humans and/or animals.

450

451 **References**

- 452 Alexandridis, P., Holzwarth, J. F., & Hatton, T. A. (1994). Micellization of Poly(ethylene oxide)-Poly(propylene
453 oxide)-Poly(ethylene oxide) Triblock Copolymers in Aqueous Solutions Thermodynamics of copolymer
454 Association. *Macromolecules*, 27, 2414–2425.
- 455 Auzély-Velty, R., & Rinaudo, M. (2003). Synthesis of starch derivatives with labile cationic groups. *International
456 Journal of Biological Macromolecules*, 31(4–5), 123–129.
- 457 Baptista, J. G. C., Rodrigues, S. P. J., Matsushita, A. F. Y., Vitorino, C., Maria, T. M. R., Burrows, H. D., ... Valente, A.
458 J. M. (2016). Does poly(vinyl alcohol) act as an amphiphilic polymer? An interaction study with simvastatin.
459 *Journal of Molecular Liquids*, 222, 287–294.
- 460 Bendoraitiene, J., Lekniute-Kyzike, E., & Rutkaite, R. (2018). Biodegradation of cross-linked and cationic starches.
461 *International Journal of Biological Macromolecules*, 119, 345–351.
- 462 Bollström, R., Tobjörk, D., Dolietis, P., Salminen, P., Preston, J., Österbacka, R., & Toivakka, M. (2013). Printability of
463 functional inks on multilayer curtain coated paper. *Chemical Engineering and Processing: Process Intensification*.
464 <https://doi.org/10.1016/j.cep.2012.07.007>
- 465 Gao, J., Luo, Z., Fu, X., Luo, F., & Peng, Z. (2012). Effect of enzymatic pretreatment on the synthesis and properties of
466 phosphorylated amphoteric starch. *Carbohydrate Polymers*, 88(3), 917–925.
467 <https://doi.org/10.1016/j.carbpol.2012.01.034>
- 468 Gigac, J., Stankovská, M., Opálená, E., & Pažitný, A. (2016). The effect of Pigments and Binders on Inkjet Print
469 Quality. *Wood Research*, 61(2), 215–226.
- 470 Gigac, J., Stankovska, M., & Pazitny, A. (2016). Influence of the Coating Formulations and Base Papers on Inkjet
471 Printability. *Wood Research*, 61(6), 915–926.
- 472 Granö, H., Yli-Kauhaluoma, J., Suortti, T., Käki, J., & Nurmi, K. (2000). Preparation of starch betainate: a novel
473 cationic starch derivative. *Carbohydrate Polymers*, 41(3), 277–283.
- 474 Haack, V., Heinze, T., Oelmeyer, G., & Kulicke, W. M. (2002). Starch derivatives of high degree of functionalization, 8
475 synthesis and flocculation behavior of cationic starch polyelectrolytes. *Macromolecular Materials and
476 Engineering*, 287(8), 495–502.
- 477 He, Z., & Alexandridis, P. (2018). Micellization thermodynamics of Pluronic P123 (EO20PO70EO20) amphiphilic
478 block copolymer in aqueous Ethylammonium nitrate (EAN) solutions. *Polymers*, 10(32).
- 479 Hebeish, A., Higazy, A., El-Shafei, A., & Sharaf, S. (2010). Synthesis of carboxymethyl cellulose (CMC) and starch-
480 based hybrids and their applications in flocculation and sizing. *Carbohydrate Polymers*, 79(1), 60–69.
- 481 Hu, G., Fu, S., Chu, F., & Lin, M. (2017). Relationship between paper whiteness and color reproduction in inkjet
482 printing. *BioResources*, 12(3), 4854–4866. <https://doi.org/10.15376/biores.12.3.4854-4866>
- 483 Huber, K. C., & BeMiller, J. N. (2001). Location of sites of reaction within starch granules. *Cereal Chemistry*, 78(2),
484 173–180. <https://doi.org/10.1094/CCHEM.2001.78.2.173>
- 485 Kasmani, J. E., Mahdavi, S., Alizadeh, A., Nemati, M., & Samariha, A. (2013). Physical properties and printability
486 characteristics of mechanical printing paper with LWC. *BioResources*, 8(3), 3646–3656.
487 <https://doi.org/10.15376/biores.8.3.3646-3656>
- 488 Lamminmäki, T. T., Kettle, J. P., & Gane, P. A. C. (2011). Absorption and adsorption of dye-based inkjet inks by
489 coating layer components and the implications for print quality. *Colloids and Surfaces A: Physicochemical and
490 Engineering Aspects*, 380(1–3), 79–88.
- 491 Lee, H. L., Shin, J. Y., Koh, C.-H., Ryu, H., Lee, D.-J., & Sohn, C. (2002). Surface sizing with cationic starch: its effect
492 on paper quality and the papermaking process. *Tappi Journal*, 1(1), 34–40.
- 493 Liu, X., Vesterinen, A. H., Genzer, J., Seppälä, J. V., & Rojas, O. J. (2011). Adsorption of PEO-PPO-PEO triblock
494 copolymers with end-capped cationic chains of poly(2-dimethylaminoethyl methacrylate). *Langmuir*.

495 <https://doi.org/10.1021/la201596x>

496 Liu, X., Wu, D., Turgman-Cohen, S., Genzer, J., Theyson, T. W., & Rojas, O. J. (2010). Adsorption of a nonionic
497 symmetric triblock copolymer on surfaces with different hydrophobicity. *Langmuir*, *26*, 9565–9574.
498 <https://doi.org/10.1021/la100156a>

499 Lourenço, A. F., Gamelas, J. A. F., Sarmiento, P., & Ferreira, P. J. T. (2020). Cellulose micro and nanofibrils as coating
500 agent for improved printability in office papers. *Cellulose*, *27*(10), 6001–6010. [https://doi.org/10.1007/s10570-](https://doi.org/10.1007/s10570-020-03184-9)
501 [020-03184-9](https://doi.org/10.1007/s10570-020-03184-9)

502 Lundberg, A., Örtengren, J., Norberg, O., & Wågberg, K. (2010). Improved print quality by surface fixation of pigments.
503 *International Conference on Digital Printing Technologies*, (February), 251–255.

504 Mujawar, L. H., Van Amerongen, A., & Norde, W. (2015). Influence of Pluronic F127 on the distribution and
505 functionality of inkjet-printed biomolecules in porous nitrocellulose substrates. *Talanta*, *131*, 541–547.
506 <https://doi.org/10.1016/j.talanta.2014.08.001>

507 Niegelhell, K., Chemelli, A., Hobisch, J., Griesser, T., Reiter, H., Hirn, U., & Spirk, S. (2018). Interaction of industrially
508 relevant cationic starches with cellulose. *Carbohydrate Polymers*, *179*, 290–296.

509 Petkova-Olsson, Y., Altun, S., Ullsten, H., & Järnström, L. (2017). Temperature effect on the complex formation
510 between Pluronic F127 and starch. *Carbohydrate Polymers*, *166*, 264–270.

511 Petkova-Olsson, Y., Ullsten, H., & Järnström, L. (2016). Thermosensitive silica-pluronic-starch model coating
512 dispersion-part I: The effect of Pluronic block copolymer adsorption on the colloidal stability and rheology.
513 *Colloids and Surfaces A: Physicochemical and Engineering Aspects*, *506*, 245–253.
514 <https://doi.org/10.1016/j.colsurfa.2016.06.032>

515 Sharma, M., Aguado, R., Murtinho, D., Valente, A. J. M., & Ferreira, P. J. T. (2021). International Journal of Biological
516 Macromolecules Novel approach on the synthesis of starch betainate by transesterification. *International Journal*
517 *of Biological Macromolecules*, *182*, 1681–1689. <https://doi.org/10.1016/j.ijbiomac.2021.05.175>

518 Sharma, M., Aguado, R., Murtinho, D., Valente, A. J. M., Mendes De Sousa, A. P., & Ferreira, P. J. T. (2020, November
519 1). A review on cationic starch and nanocellulose as paper coating components. *International Journal of*
520 *Biological Macromolecules*, Vol. 162, pp. 578–598. <https://doi.org/10.1016/j.ijbiomac.2020.06.131>

521 Shi, H., Liu, H., Ni, Y., Yuan, Z., Zou, X., & Zhou, Y. (2012). Review: Use of optical brightening agents (OBAs) in the
522 production of paper containing high-yield pulps. *BioResources*, *7*(2), 2582–2591.
523 <https://doi.org/10.15376/biores.7.2.2582-2591>

524 Sousa, S., De Sousa, A. M., Reis, B., & Ramos, A. (2014). Influence of Binders on Inkjet Print Quality. *Materials*
525 *Science*, *20*(1). <https://doi.org/10.5755/j01.ms.20.1.1998>

526 Stankovská, M., Gigac, J., Letko, M., & Opálená, E. (2014). The Effect of Surface Sizing on Paper Wettability and on
527 Properties of Inkjet Prints. *Wood Research*, *59*(1), 67–76.

528 Thapa, R. K., Cazzador, F., Grønlien, K. G., & Tønnesen, H. H. (2020). Effect of curcumin and cosolvents on the
529 micellization of Pluronic F127 in aqueous solution. *Colloids and Surfaces B: Biointerfaces*, *195*(July 2020).
530 <https://doi.org/10.1016/j.colsurfb.2020.111250>

531 Wang, S., & Cheng, Q. (2009). A novel process to isolate fibrils from cellulose fibers by high-intensity ultrasonication,
532 Part 1: Process optimization. *Journal of Applied Polymer Science*, *113*(2), 1270–1275.
533